



ISSN: 0067-2904

## Bifurcation and Stability Analysis of Stagnation Point for Fluid Flow in an Inclined Channel with Inclined Magnetic Field for Peristaltic Transport

Hatem Nahi Mohaisen<sup>1\*</sup>, Ahmad M. Abdulhadi<sup>2</sup>, Rasha M. Yaseen<sup>3</sup>

<sup>1</sup>Department of Mathematic, Minister's office, Ministry of High Education and Scientific Research, Iraq

<sup>2</sup>Department of Mathematics, College of Science, University of Baghdad, Iraq

<sup>3</sup>Department of Biomedical Eng., Al-Khwarizmi College of Engineering, University of Baghdad, Iraq

Received: 19/3/2023

Accepted: 1/5/2023

Published: 30/5/2024

### Abstract

Streamlined peristaltic transport patterns, bifurcations of equilibrium points, and effects of an inclined magnetic field and channel are shown in this study. The incompressible fluid has been the subject of the model's investigation. The Reynolds values for evanescence and an infinite wavelength are used to constrain the flow while it is being studied in a slanted channel with a slanted magnetic field. The topologies over their domestic and cosmopolitan bifurcations are investigated for the outcomes, and notion of the dynamical system are employed. The Mathematica software is used to solve the nonlinear autonomous system. The flow is found to have three different flow distributions namely augmented, trapping and backward flow. Outcomes are graphically represented along with a number of parameters that have an impact on how the fluid behaves when flowing with bifurcations.

**Keywords:** Nonlinear Autonomous System, bifurcations, Streamline, Peristaltic Transport, Inclined Channel, Inclined Magnetic.

## تحليل التشعب والاستقرار لنقطة الركود لتدفق السوائل في قناة مائلة مع مجال مغناطيسي مائل للنقل التمعجي

حاتم ناهي محيسن<sup>1\*</sup>، احمد مولود عبد الهادي<sup>2</sup>، رشا حميد ياسين<sup>3</sup>

<sup>1</sup>قسم الرياضيات، مكتب الوزير، وزارة التعليم العالي والبحث العلمي، بغداد، العراق.

<sup>2</sup>قسم الرياضيات، كلية العلوم، جامعة بغداد، العراق.

<sup>3</sup>قسم الهندسة الطبية الحيوية، كلية الهندسة الخوارزمي، جامعة بغداد، العراق.

### الخلاصة

تم عرض أنماط النقل التمعجية المبسطة، وتشعبات نقاط التوازن، وتأثيرات المجال المغناطيسي المائل والقناة في هذه الدراسة. كان السائل غير القابل للضغط موضوع تحقيق النموذج. يتم فحص التدفق في قناة مائلة ذات مجال مغناطيسي مائل بينما يتم تقييده بواسطة أرقام رينولدز للتلاشي وطول موجة لانهازي. باستخدام نظرية النظام الديناميكي، تمت دراسة الطوبولوجيا على طول التشعبات المحلية والعالمية للحصول على النتائج. تم استخدام برنامج Mathematica لحل النظام المستقل غير الخطي. تم تحديد ثلاثة توزيعات

\*Email: [ha19652010@yahoo.com](mailto:ha19652010@yahoo.com)

تدفق بديلة في التدفق: التدفق المعزز ، وتدفق الملاحة ، والتدفق العكسي. يتم تمثيل النتائج بيانياً إلى جانب عدد من المعلمات التي لها تأثير على كيفية تصرف المائع عند التدفق مع التشعبات.

## 1. Introduction

One of the primary fluid-transporting mechanisms in the physiological systems of mammals, including humans, is the peristaltic. This system controls the flow of liquid lymph through lymphatic arteries, the transport of spermatozoa in the citation male reproductive tract, and the movement of pee from the kidney to the bladder through the ureter. With devices, such as heart-lung contrivances, peristaltic insufflation that works on the same principle, is also utilized to pump blood. In a tube or channel, this mechanism is produced by the movement of the walls. To understand peristaltic transfer in both mechanical and physiological states according to different assumptions, many empirical and theoretical research have been conducted. Shapiro AH. et al. [1] presented the peristaltic transfer under an infinite wavelength approximation in a range of motion for Newtonian fluids. Mohaisen H.N. et al. [2] presented the peristaltic flow of a two-dimensional Bingham plastic fluid under the influence of the heat transfer, rotation, and an induced magnetic field. Nadeem S. et al. [3] studied the peristaltic flows in an inclined asymmetric and symmetric channel is affected by the inclined magnetic field of the Williamson fluid model. Farah A. et al. [4] investigated the effects of an inclined magnetic field on the peristaltic transport of incompressible Bingham plastic fluid with heat transfer and mass transfer in an inclined symmetric channel. The heat transfer and concentration slip conditions are used. Kaleem U. et al. [5] proposed a work to investigate the stability of critical to stagnation points, streamline topologies, and their domestic and cosmopolitan bifurcations for peristaltic flow of an incompressible power-law model. F. G URCAN. et al. [6] studied the streamline styles and their bifurcations in 2-dimensional Navier-Stokes flow of an incompressible fluid close a non-simple degenerate critical point near a stationary which is examined from a topological point of view by accounting for a Taylor expansion of the velocity domain. Gürcan F. et al. [7] examined the streamline styles and their bifurcations at straightforward, off-the-boundary degenerate critical points in a two-dimensional, and incompressible fluid. Morten BRØNS [8], analyse the structures of vortices and separation in the streamlined patterns of fluid flows using dynamical systems theory. By using normal form simplifications, the bifurcation of patterns under variation in external parameters is examined. D E L A. et al. [9] presented the symmetric condition about a straight line is used to explore local flow patterns and their bifurcations associated with non-simple degenerate critical points that emerge distant from boundaries. Joel Jiménez. et al. [10] studied the streamline styles and their domestic and cosmopolitan bifurcations in a two-dimensional planar surface and axisymmetric peristaltic flow for an incompressible Newtonian fluid. Under the conditions of a long-wavelength and low-Reynolds number approximation, the stream-function has an analytical solution. Asghar Z. et al. [11] evaluated the streamline styles and their bifurcations for a Newtonian fluid flowing with heat transfer in an unsettled convective and peristaltic manner. The flow is analysed in a two-dimensional symmetric channel under the widely agreeable presumptions of an infinite wavelength and a depressed Reynolds number in a wave framework of reference. Ullah K. et al., [12] the stability of equilibrium points and their bifurcations for a peristaltic transfer of an incompressible viscous fluid through an inclined channel have been studied when the channel width is supposed to be very small in comparison to the peristaltic wave wavelength and inertial impacts are negligible. Sadia et al. [13] used the dynamical system approach in the investigations in order to explore the streamlined patterns along their bifurcations for peristaltic flow under mixed convection effects. Both an axisymmetric tube and a two-dimensional symmetric channel are taken into consideration for the flow. Nasir A. et al. [14] utilized a power-law model to test the bifurcations of equilibrium points and their streamlined styles for the peristaltic outflow of fluids that are shear-thinning and shear-

thickening over an asymmetric canal. Under the presumptions of the vanishing Reynolds number and infinite wavelength approximations, a precise solution in the wave framework of reference is obtained. Ehsan T. et al. [15] studies the use of a novel method to identify distinctive peristaltic flow features like bolus and trapping. By employing dynamic system analysis, we link the incident of a bolus to the existence of a centre (an elliptic critical point) when centres are presented beneath the wave crests and a pair of saddles (hyperbolic equilibrium points) are located on the central line, trapping. Jagdeesh V. et al. [16] presented how an inclined non-uniform channel's inclined magnetic field, porous medium, and wall characteristics affect the peristaltic transport of the Jeffery fluid. Ullah K. et al. [17] studied the peristaltic transport of viscoelastic fluid through an axisymmetric tub. The bifurcation analysis is carried out to investigate the qualitative character of stagnation spots and different flow zones.

In this study, the way of the issue is handled mathematically, the precise location and behaviour of stagnation points, as well as their bifurcations, are described by a dynamical system. In addition, when the magnetic field and channel are inclined, we evaluate different flow zones and their ranges using global bifurcation diagrams. This is done by presenting a set of graphs for the many factors influencing the peristaltic transfer of a fluid.

**2. Mathematical formulation of issue**

Imagine that an incompressible fluid flows along an inclined channel while being subjected to an inclined magnetic field. A two-dimensional symmetrical channel is filled with fluid. Along the channel's edges, sine waves propagate at a constant speed (c). We select a  $(\bar{X}, \bar{Y})$  rectangular coordinate system for the channel with  $\bar{X}$  is along the centerline and  $\bar{Y}$  transverses to the spread way of waves. The geometry of the canal walls is described in Figure 1.

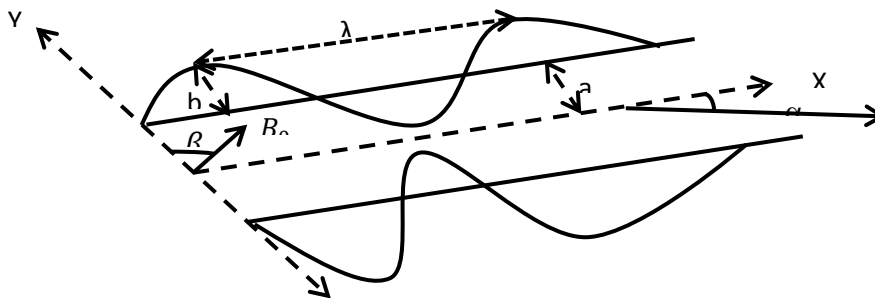


**Figure 1:** Geomtrv of the issue

It is given by:

$$H(\bar{X}, \bar{t}) = a + b(1 - \text{Cos}^2(\frac{\pi}{\lambda}(\bar{X} - c\bar{t}))) \tag{1}$$

Where a, b, c,  $\bar{t}$  and  $\lambda$  are the width of the wave, amplitude wave, speed of wave, time and wavelength, respectively. The Cauchy stress tensor ( $\bar{\tau}$ ) for viscous fluid is

$$\bar{\tau} = -\bar{P}\bar{I} + \mu\bar{\gamma} \tag{2}$$

Where  $\mu, \bar{P}$ , and  $\bar{I}$  are the viscosity, pressure, identity tensor respectively. We define  $\bar{\gamma}$  as follows:

$$\bar{\gamma} = (\text{grad } \bar{V}) + ((\text{grad } \bar{V})^T) \tag{3}$$

Where T is the creation of the transposition and  $\bar{V}$  is the vector of velocity. In experimenter form  $(\bar{X}, \bar{Y})$ , the prevailing equations can be expressed as follows:

$$\frac{\partial \bar{U}}{\partial \bar{X}} + \frac{\partial \bar{V}}{\partial \bar{Y}} = 0, \tag{4}$$

$$\rho \left( \frac{\partial}{\partial \bar{t}} + \bar{U} \frac{\partial \bar{U}}{\partial \bar{x}} + \bar{V} \frac{\partial \bar{U}}{\partial \bar{y}} \right) = -\frac{\partial \bar{P}}{\partial \bar{x}} + \mu \left( \frac{\partial^2 \bar{U}}{\partial \bar{x}^2} + \frac{\partial^2 \bar{U}}{\partial \bar{y}^2} \right) - \sigma B_0^2 \text{Cos}(\beta) (\bar{U} \text{Cos}(\beta) - \bar{V} \text{Sin}(\beta)) + \rho g \text{Sin}(\alpha) \tag{5}$$

$$\rho \left( \frac{\partial}{\partial \bar{t}} + \bar{U} \frac{\partial \bar{V}}{\partial \bar{x}} + \bar{V} \frac{\partial \bar{V}}{\partial \bar{y}} \right) = -\frac{\partial \bar{P}}{\partial \bar{y}} + \mu \left( \frac{\partial^2 \bar{V}}{\partial \bar{x}^2} + \frac{\partial^2 \bar{V}}{\partial \bar{y}^2} \right) + \sigma B_0^2 \text{Cos}(\beta) (\bar{U} \text{Cos}(\beta) - \bar{V} \text{Sin}(\beta)) - \rho g \text{Sin}(\alpha) \tag{6}$$

Where  $\bar{U}$  and  $\bar{V}$  represent the velocity compounds in  $\bar{X}$  and  $\bar{Y}$  orientations, respectively,  $\rho$  is the density of the fluid,  $\bar{t}$  is the time,  $\sigma$  is electrical conductivity,  $B_0$  is the strength of the magnetic field,  $\bar{P}$  is the pressure,  $\mu$  is the viscosity, the gravitational acceleration is  $g$ , the magnetic field's slanted angle is  $\beta$ , while the slanted channel is  $\alpha$ . The following conversions can be employed to come in a wave framework of reference  $(\bar{x}, \bar{y})$  that concerns to the fixed framework of the reference and get about with the speed of  $c$  for steady flow:

$$\bar{x} = \bar{X} - c\bar{t}, \bar{Y} = \bar{y}, \bar{u} = \bar{U} - c, \bar{v} = \bar{V}, \bar{P} = \bar{p}. \tag{7}$$

The terms  $\bar{u}, \bar{v}$  and  $\bar{p}$  stand for the velocity compounds and pressure in wave framework. Now, the dimensionless variables and parameters are described as follows:

$$x = \frac{\bar{x}}{\lambda}, y = \bar{y}/a, \bar{u} = uc, \delta = \frac{a}{\lambda}, \bar{v} = vc\delta, \bar{t} = \frac{t\lambda}{c}, \phi = \frac{b}{a}, M^2 = \frac{\sigma B_0^2 a^2}{\mu}, R_e = \frac{\rho ca}{\mu}, \bar{p} = \frac{p\mu c\lambda}{a^2}, \omega = \frac{\rho g a^2}{\mu c}, h = \frac{\bar{H}}{a} \tag{8}$$

Where  $R_e$  is the Reynold number,  $M$  is the Hartman number,  $\delta$  is the wave rate and  $\phi$  is the amplitude ratio. Substituting equation (8) with help equation (7) in equation 1, 4, 5 and 6. The equation (4) is identically satisfied and simplify the result and. When the values of  $(R_e \ll 1$  and  $\delta \ll 1)$  we obtain the following:

$$h=1-\phi(1 - \text{Cos}^2(x)) \tag{9}$$

$$\frac{\partial p}{\partial x} = \frac{\partial^2 u}{\partial y^2} - M^2 \text{Cos}^2(\beta)u + \omega \text{Sin}(\alpha) \tag{10}$$

$$\frac{\partial p}{\partial y} = 0 \tag{11}$$

We specify the stream function as follows:

$$u = \frac{\partial \psi}{\partial y} \text{ and } v = -\frac{\partial \psi}{\partial x} \tag{12}$$

Following the cross differentiation for the pressure gradient of equations 10, and 11 to be eliminated, we obtain:

$$\frac{\partial^4 \psi}{\partial y^4} - M^2 \text{Cos}^2(\beta) \frac{\partial^2 \psi}{\partial y^2} = 0 \tag{13}$$

The wave frame of volume flow rate and boundary cases without dimensional are as follows:

$$\psi = 0, \frac{\partial^2 \psi}{\partial y^2} = 0, \text{ when } y=0, \tag{14a}$$

$$\psi = q, \frac{\partial \psi}{\partial y} = -1, \text{ when } y=h, \tag{14b}$$

$$q = \int_0^h \frac{\partial \psi}{\partial y} dy = \psi(h) - \psi(0). \tag{15}$$

### 3. Solution to the issue

Equation (13) satisfies the boundary requirements in equations (14a) and (14b):

$$\psi(x, y) = \frac{\sqrt{A}qy \text{Cosh}[\sqrt{A}h] + y \text{Sinh}[\sqrt{A}h] - (q+h) \text{Sinh}[\sqrt{A}y]}{\sqrt{A}h \text{Cosh}[\sqrt{A}h] - \text{Sinh}[\sqrt{A}h]} \tag{16}$$

Where  $A = M^2 * (\text{Cos}[\beta])^2$

Backward flow, trapping, and augmented flow are three different flow situations that might occur [1, 18]. When a flow is said to be flowing backward, the entire flow is moves in the opposite direction. Trapping is the phenomenon in which a closed streamline splinter to enclose a bolus of fluid particles. The augment occurs when the constrained bolus is divided into multiple streams of flow and moves ahead. Figure 2 illustrates these flow conditions.

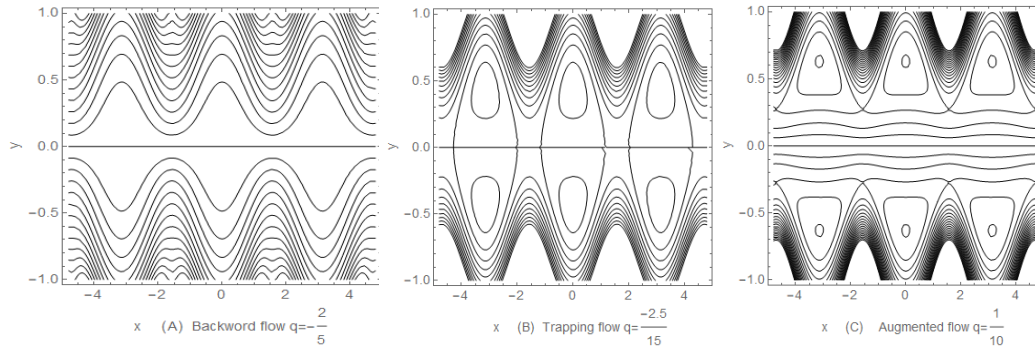


**Figure 2:** Streamline for various q values with

**4. The Non-linear Dynamical System of the Flow Field**

This portion, examine variations in flow demean and ideas from the specific theory of dynamical systems will be used. Individual particle instantaneous motion (say  $t = t_0$ ), movement along lines are indicated by  $\dot{x} = V(x, t_0)$ . The system of non-linear autonomous differental equations can be employed to describe the current issue as follows.

$\dot{x} = \partial\psi/\partial y$  and  $\dot{y} = -\frac{\partial\psi}{\partial x}$ . From equation (16), we have

$$\dot{x} = \frac{\sqrt{A}(q\text{Cosh}[\sqrt{A}h] - (q+h)\text{Cosh}[\sqrt{A}y]) + \text{Sinh}[\sqrt{A}h]}{\sqrt{A}h\text{Cosh}[\sqrt{A}h] - \text{Sinh}[\sqrt{A}h]} = f(x, y, \varphi). \tag{17}$$

$$\dot{y} = \frac{(-2Ayh + 2\sqrt{A}\text{Cosh}[\sqrt{A}h]h\text{Sinh}[\sqrt{A}y] - 2(1+Ah(q+h))\text{Sinh}[\sqrt{A}y]\text{Sinh}[\sqrt{A}h] + 2Aqy\text{Sinh}[\sqrt{A}h]^2 + \sqrt{A}y\text{Sinh}[2\sqrt{A}h])h1}{2(-\sqrt{A}\text{Cosh}[\sqrt{A}h]h + \text{Sinh}[\sqrt{A}h])^2} = g(x, y, \varphi) \tag{18}$$

Where  $h = 1 - \phi * (1 - \text{Cos}[x]^2)$  and  $h1 = \frac{\partial h}{\partial x}$ .

Where  $x = \{x, y, \varphi\}$  is the coordinates in space and  $\varphi = \{\phi, q, M, \beta\}$  are the parameters. The value of the amplitude ratio spans from 0 to 1, moreover, the area of interest is  $-\infty < x < \infty$  and  $-h < y < h$ .

By applying the Hartman-Grobman theorem, which claims that equilibrium points of the Jacobian may be utilized to identify its characteristics, first, we set  $f(x, y, \varphi) = g(x, y, \varphi) = 0$  by doing as stated in [10]. If the determinant of the Jacobian at a given location is zero, the point is degenerate. Simple and non-simple degeneracies are two of their subclasses. A simple degeneracy exists when the eigenvalues of the Jacobian matrix are equal to zero. For a non-simple degeneracy, the Jacobian matrix is equal to zero. To categorize the important points, we will use the same notations that are used in [19]. Where the trace  $P_{12} = \lambda_1 + \lambda_2$  and the Jacobian  $d_{12} = \lambda_1 * \lambda_2$ , which are based on the eigenvalues  $\lambda_1$  and  $\lambda_2$ . To classify them, we use the phase pictures, classify.

A bifurcation point with respect to the parameter, claims [20] is the solution  $(x, y, \varphi)$ , and when passes through  $\varphi_c$ , with  $\varphi_c$  as critical value, the quantity of periodic, quasi-periodic, or equilibrium solutions varies.

The critical points are given by:

1.  $\{x_{1,2}, y_{1,2}\} = \left\{ n\pi, \pm \frac{\text{ArcCosh}\left[\frac{q\text{Cosh}[\sqrt{A}] + \frac{\text{Sinh}[\sqrt{A}]}{\sqrt{A}}}{1+q}\right]}{\sqrt{A}} \right\}, n \in Z;$
2.  $\{x_{3,4}, y_{3,4}\} = \left\{ \pm \frac{\sqrt{\sqrt{A}(-1-q+q\text{Cosh}[\sqrt{A}]) + \text{Sinh}[\sqrt{A}]}}{\sqrt{\sqrt{A}\phi(-1+\text{Cosh}[\sqrt{A}]) + Aq\phi\text{Sinh}[\sqrt{A}]}} \right\}, 0\}$

3.

$$4. \quad \{x_{5,6}, y_{5,6}\} = \left\{ \frac{(2n-1)\pi}{2}, \pm \frac{\text{ArcCosh}\left[\frac{q\text{Cosh}[\sqrt{A}(-1+\phi)] + \frac{\text{Sinh}[\sqrt{A}(1-\phi)]}{\sqrt{A}}}{1+q-\phi}\right]}{\sqrt{A}} \right\}, n \in Z.$$

**5. Critical points classification and bifurcation**

A. The point critical:

$$\{x_{1,2}, y_{1,2}\} = \left\{ n\pi, \pm \frac{\text{ArcCosh}\left[\frac{q\text{Cosh}[\sqrt{A}] + \frac{\text{Sinh}[\sqrt{A}]}{\sqrt{A}}}{1+q}\right]}{\sqrt{A}} \right\}$$

Where  $n \in Z$ , the equilibrium point lies under the wave crests. At these equilibrium points, the Jacobian matrix is:

$$\begin{aligned} qq1 &= \sqrt{\frac{-\sqrt{A}(1+q) + \sqrt{A}q \cosh[\sqrt{A}] + \sinh[\sqrt{A}]}{\sqrt{A}(1+q) + \sqrt{A}q \cosh[\sqrt{A}] + \sinh[\sqrt{A}]}} \\ qq2 &= \sqrt{A}(1+q) + \sqrt{A}q \cosh[\sqrt{A}] + \sinh[\sqrt{A}] \\ qq3 &= (q \cosh \sqrt{A} + \sinh[\sqrt{A}]/\sqrt{A})/(1+q) \\ z &= -\phi \left( \frac{1}{(-\sqrt{A} \cosh[\sqrt{A}] + \sinh[\sqrt{A}])^2} \right) \end{aligned}$$

$$z1 = -2\sqrt{A} \cosh^{-1}[qq3] + 2\sqrt{A}q \cosh^{-1}[qq3] \sinh[\sqrt{A}]^2,$$

$$z2 = \frac{2\text{Cosh}[\sqrt{A}]qq1qq2}{1+q} - \frac{2(1+A+q)\text{Sinh}[\sqrt{A}]qq1(1+q+q\text{Cosh}[\sqrt{A}] + \frac{\text{Sinh}[\sqrt{A}]}{\sqrt{A}})}{1+q},$$

$$z3 = \text{ArcCosh}[qq3]\text{Sinh}[2\sqrt{A}]$$

$$J \setminus \{x_{1,2}, y_{1,2}\} = \begin{bmatrix} 0 & -\frac{(\sqrt{A}qq1qq2)}{(\sqrt{A} \cosh[\sqrt{A}] - \sinh[\sqrt{A}])} \\ z(z1+z2+z3) & 0 \end{bmatrix},$$

$$\lambda_{12} = \pm \frac{\sqrt{A}qq1qq2z[z1+z2-z3]}{\sqrt{\sqrt{A}qq1qq2(-\sqrt{A}\text{Cosh}[\sqrt{A}] + \text{Sinh}[\sqrt{A}])z[z1+z2-z3]}}$$

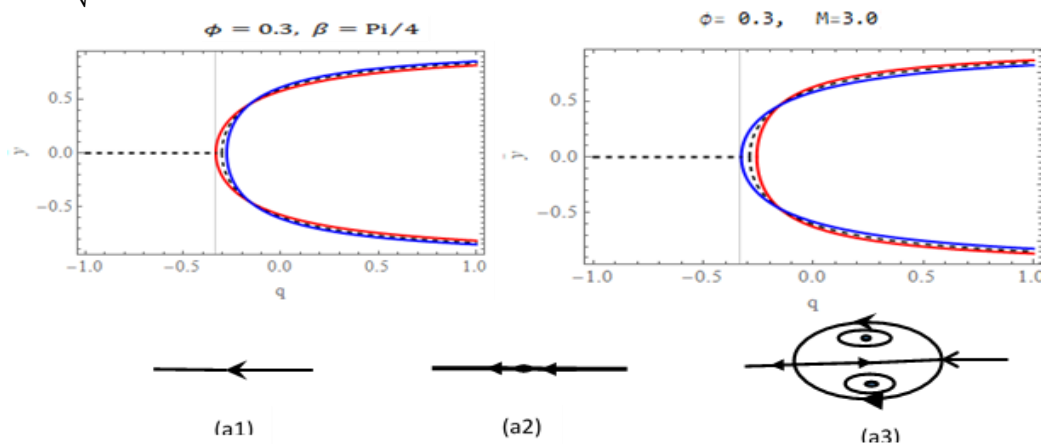


**Figure 3.** Bifurcation diagrams for critical point lie on vertical line below of the wave crest  $x = n\pi$  and topological changes (a1)  $q < \frac{1 - \frac{\text{Sinh}[\sqrt{A}]}{\sqrt{A}}}{-1 + \text{Cosh}[\sqrt{A}]}$ , (a2)  $q = \frac{1 - \frac{\text{Sinh}[\sqrt{A}]}{\sqrt{A}}}{-1 + \text{Cosh}[\sqrt{A}]}$ , (a3)  $q > \frac{1 - \frac{\text{Sinh}[\sqrt{A}]}{\sqrt{A}}}{-1 + \text{Cosh}[\sqrt{A}]}$

The eigenvalues change with flow rate  $q$  at fixed values of  $\phi$ ,  $\beta$  and  $M$ . The flow rate is specified to be between -1 and 1. As a result, the temperament and stability of the equilibrium points alter with flow rate  $q$ .

- For critical value  $q = \frac{1 - \frac{\text{Sinh}[\sqrt{A}]}{\sqrt{A}}}{-1 + \text{Cosh}[\sqrt{A}]}$ , there is an isolated critical point that is neither a simple degeneracy nor a point of hyperbolic degeneration, since  $J_{x_{12}, y_{1,2}} = 0$ . See Figure (3.a2).
- It is referred to the stagnation point as a stable centre for  $q > \frac{1 - \frac{\text{Sinh}[\sqrt{A}]}{\sqrt{A}}}{-1 + \text{Cosh}[\sqrt{A}]}$ , and  $p_{12} = 0$  and  $d_{12} > 0$ , see Figure (3.a3).

**B. The critical point:**

$$\{x_{3,4}, y_{3,4}\} = \left\{ \pm \frac{\sqrt{\sqrt{A}(-1-q+q\text{Cosh}[\sqrt{A}]) + \text{Sinh}[\sqrt{A}]}}{\sqrt{\sqrt{A}\phi(-1+\text{Cosh}[\sqrt{A}]) + Aq\phi\text{Sinh}[\sqrt{A}]}} , 0 \right\};$$

On the channel's centreline, this critical point is located. At this critical point, the Jacobian is given as follows:

$$qq4 = \frac{2\sqrt{-\sqrt{A}(1+q) + \sqrt{A}q\text{Cosh}[\sqrt{A}] + \text{Sinh}[\sqrt{A}]}}{\sqrt{\sqrt{A}\phi(-1+\text{Cosh}[\sqrt{A}]) + \sqrt{A}q\phi\text{Sinh}[\sqrt{A}]}};$$

$$qq5 = \frac{\sqrt{\sqrt{A}(-1-q+q\text{Cosh}[\sqrt{A}]) + \text{Sinh}[\sqrt{A}]}}{\sqrt{\sqrt{A}\phi(-1+\text{Cosh}[\sqrt{A}]) + Aq\phi\text{Sinh}[\sqrt{A}]}};$$

$$x1 = -2\sqrt{A}\phi\text{Sin}[qq4]\text{Sinh}\left[\frac{1}{4}\sqrt{A}(2 - \phi + \phi\text{Cos}[qq4])\right](\sqrt{A}q\text{Cosh}\left[\frac{1}{4}\sqrt{A}(2 - \phi + \phi\text{Cos}[qq4])\right] + \text{Sinh}\left[\frac{1}{4}\sqrt{A}(2 - \phi + \phi\text{Cos}[qq4])\right]);$$

$$x2 = (\sqrt{A}(1 - \phi + \phi\text{Cos}[qq5]^2)\text{Cosh}[\sqrt{A}(1 - \phi + \phi\text{Cos}[qq5]^2)] - \text{Sinh}[\sqrt{A}(1 - \phi + \phi\text{Cos}[qq5]^2)]);$$

$$x3 = 2A\phi\text{Cos}[qq5](1 - \phi + \phi\text{Cos}[qq5]^2)\text{Sin}[qq5]\text{Sinh}[\sqrt{A}(1 - \phi + \phi\text{Cos}[qq5]^2)];$$

$$x4 = (\sqrt{A}(-1 - q + \phi - \phi\text{Cos}[qq5]^2 + q\text{Cosh}[\sqrt{A}(1 - \phi + \phi\text{Cos}[qq5]^2)]) + \text{Sinh}[\sqrt{A}(1 - \phi + \phi\text{Cos}[qq5]^2)]);$$

$$x5 = (-\sqrt{A}(1 - \phi + \phi\text{Cos}[qq5]^2)\text{Cosh}[\sqrt{A}(1 - \phi + \phi\text{Cos}[qq5]^2)] + \text{Sinh}[\sqrt{A}(1 - \phi + \phi\text{Cos}[qq5]^2)])^2;$$

$$x6 = -2A(1 - \phi + \phi\text{Cos}[qq5]^2) + 2A(1 - \phi + \phi\text{Cos}[qq5]^2)\text{Cosh}[\sqrt{A}(1 - \phi + \phi\text{Cos}[qq5]^2)];$$

$$x7 = 2\sqrt{A}(1 + A(1 - \phi + \phi\text{Cos}[qq5]^2)(1 + q - \phi + \phi\text{Cos}[qq5]^2))\text{Sinh}[\sqrt{A}(1 - \phi + \phi\text{Cos}[qq5]^2)];$$

$$x8 = 2Aq\text{Sinh}[\sqrt{A}(1 - \phi + \phi\text{Cos}[qq5]^2)]^2 + \sqrt{A}\text{Sinh}[2\sqrt{A}(1 - \phi + \phi\text{Cos}[qq5]^2)];$$

$$x9 = -\sqrt{A}(1 - \phi + \phi\text{Cos}[qq5]^2)\text{Cosh}[\sqrt{A}(1 - \phi + \phi\text{Cos}[qq5]^2)] + \text{Sinh}[\sqrt{A}(1 - \phi + \phi\text{Cos}[qq5]^2)];$$

$$J_{(x_{3,4}, y_{3,4})} = \begin{bmatrix} (x1 * x2 + x3 * x4)/x5 & 0 \\ 0 & -((\phi\text{Cos}[qq5]\text{Sin}[qq5](x6 - x7 + x8))/(x9^2)) \end{bmatrix};$$

With the eigenvalues:

$$\lambda_{22} = \pm \frac{x1x2+x3x4}{x5}; \lambda_{23} = \pm \left(-\frac{(x6-x7+x8)\text{Sin}[qq5]\phi\text{Cos}[qq5]}{x9^2}\right);$$

Since, the critical points,  $\{x_{3,4}, y_{3,4}\}$ , change their behavior in the range  $\frac{1 - \frac{\text{Sinh}[\sqrt{A}]}{\sqrt{A}}}{-1 + \text{Cosh}[\sqrt{A}]} < q < \frac{-4 + \phi \text{ArcCos}[\frac{-2+\phi}{\phi}]^2 + \phi \text{ArcCosh}[\frac{-2+\phi}{\phi}]^2 \text{Cosh}[\sqrt{A}] + \frac{4\text{Sinh}[\sqrt{A}]}{\sqrt{A}}}{4 - 4\text{Cosh}[\sqrt{A}] + \sqrt{A}\phi \text{ArcCos}[\frac{-2+\phi}{\phi}]^2 \text{Sinh}[\sqrt{A}]}$ , In this range, their temperament and stability are examined. These are two critical event  $q = q_{c_1} = \frac{1 - \frac{\text{Sinh}[\sqrt{A}]}{\sqrt{A}}}{-1 + \text{Cosh}[\sqrt{A}]}$  and  $q = q_{c_2} = \frac{-4 + \phi \text{ArcCos}[\frac{-2+\phi}{\phi}]^2 + \phi \text{ArcCosh}[\frac{-2+\phi}{\phi}]^2 \text{Cosh}[\sqrt{A}] + \frac{4\text{Sinh}[\sqrt{A}]}{\sqrt{A}}}{4 - 4\text{Cosh}[\sqrt{A}] + \sqrt{A}\phi \text{ArcCos}[\frac{-2+\phi}{\phi}]^2 \text{Sinh}[\sqrt{A}]}$  occur.

The following qualitative alters can be seen:

- When  $q = q_{c_1} = \frac{1 - \frac{\text{Sinh}[\sqrt{A}]}{\sqrt{A}}}{-1 + \text{Cosh}[\sqrt{A}]}$ ,  $q = q_{c_2} = \frac{-4 + \phi \text{ArcCos}[\frac{-2+\phi}{\phi}]^2 + \phi \text{ArcCosh}[\frac{-2+\phi}{\phi}]^2 \text{Cosh}[\sqrt{A}] + \frac{4\text{Sinh}[\sqrt{A}]}{\sqrt{A}}}{4 - 4\text{Cosh}[\sqrt{A}] + \sqrt{A}\phi \text{ArcCos}[\frac{-2+\phi}{\phi}]^2 \text{Sinh}[\sqrt{A}]}$ , the  $p_{34}$  and  $d_{34} = 0$ . For equilibrium points, which are non-hyperbolic decadent sites with non-simple decadent, the Jacobian matrix and the eigenvalues are 0; see Figures (4.a, 4c).
- When  $q_{c_1} < q < q_{c_2}$ , the stagnation points are referred as saddle nodes, because that  $p_{34} = 0$  and  $d_{34} < 0$ . See Figure (4.b).

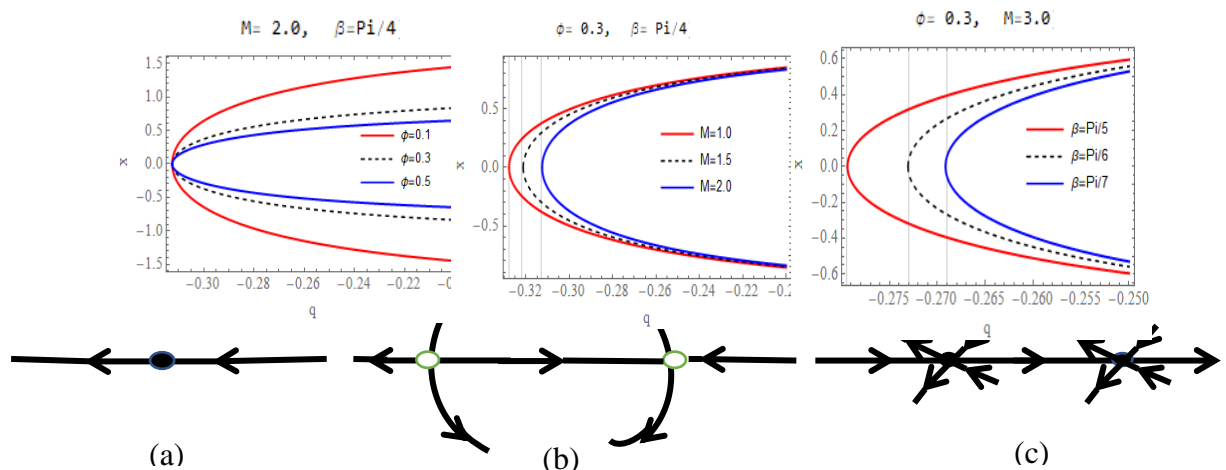


**Figure 4:** Bifurcation diagrams for critical points lie on centreline of channel, and the topology changes: (a)

**C. The critical point:**

$$\{x_{5,6}, y_{5,6}\} = \left\{ \frac{(2n-1)\pi}{2}, \pm \frac{\text{ArcCosh}\left[\frac{q \text{Cosh}[\sqrt{A}(-1+\phi)] + \frac{\text{Sinh}[\sqrt{A}(1-\phi)]}{\sqrt{A}}}{1+q-\phi}\right]}{\sqrt{A}} \right\}, n \in Z.$$

This critical point is located below the wave troughs on the vertical. The Jacobian presented by:

$$Aq = (\sqrt{A}(1+q-\phi)qq2\sqrt{1 - \frac{2\sqrt{A}(1+q)}{qq2}})/((1+q)(\sqrt{A}(-1+\phi)\text{Cosh}[\sqrt{A}(-1+\phi)] + \text{Sinh}[\sqrt{A}(1-\phi)]))$$

$$Aq1 =$$

$$(\phi(2\sqrt{A}(-1 + \phi)\text{ArcCosh}[qq3] - \frac{2(-1+\phi)\text{Cosh}[\sqrt{A}(-1+\phi)]qq1qq2}{1+F} - \frac{1}{1+F} 2(1 + A(-1 + \phi)(-1 - F + \phi))qq1(1 + F + F\text{Cosh}[\sqrt{A}] + \frac{\text{Sinh}[\sqrt{A}]}{\sqrt{A}})\text{Sinh}[\sqrt{A}(1 - \phi)] + 2\sqrt{A}F\text{ArcCosh}[qq3]\text{Sinh}[\sqrt{A}(1 - \phi)]^2 + \text{ArcCosh}[qq3]\text{Sinh}[2\sqrt{A}(1 - \phi)])) ,$$

$$Aq2=(\sqrt{A}(-1 + \phi)\text{Cosh}[\sqrt{A}(-1 + \phi)] + \text{Sinh}[\sqrt{A}(1 - \phi)])^2$$

$$Aq3=Aq1/Aq2$$

$$J_{x_{5,6},y_{5,6}} = \begin{bmatrix} 0 & Aq \\ Aq3 & 0 \end{bmatrix};$$

The eigenvalues are:

$$Aq4=(\sqrt{-A}\sqrt{1 - \frac{2\sqrt{A}(1+F)}{qq2}}qq2(1 + F - \phi)\phi(\sqrt{A}(-1 + \phi)\text{Cosh}[\sqrt{A}(-1 + \phi)] - \text{Sinh}[\sqrt{A}(-1 + \phi)])(2qq1(\sqrt{A}qq2(-1 + \phi)\text{Cosh}[\sqrt{A}(-1 + \phi)] + (-1 + A(1 + F - \phi)(-1 + \phi))(\sqrt{A}(1 + F + F\text{Cosh}[\sqrt{A}]) + \text{Sinh}[\sqrt{A}])\text{Sinh}[\sqrt{A}(-1 + \phi)] + \sqrt{A}(1 + F)\text{ArcCosh}[qq3](\sqrt{A}(2 + F - 2\phi - F\text{Cosh}[2\sqrt{A}(-1 + \phi)]) + \text{Sinh}[2\sqrt{A}(-1 + \phi)]))))) ;$$

$$Aq5=(\sqrt{A}(1 + F)(\sqrt{A}(-1 + \phi)\text{Cosh}[\sqrt{A}(-1 + \phi)] + \text{Sinh}[\sqrt{A}(1 - \phi)]))^2 ;$$

$$\lambda_{56} = \pm(\frac{Aq4}{Aq5}) ;$$

Since, the equilibrium is qualitative changes in their behavior between the  $q_{c5} < q < q_{c6}$

where,  $q_{c5} = -1 + \phi$  and  $q_{c6} = -\frac{1 + \frac{\text{Sinh}[\sqrt{A}]}{\sqrt{A}}}{1 + \text{Cosh}[\sqrt{A}]}$ .

- When,  $q=q_{c5} = q_{c6}$  then  $d_{56} = p_{56} = 0$ . Therefore, the Jacobian matrix has zeroed out, creating a non-hyperbolic decadent point at the slump point that correlates to non-simple decadence; see Figure (5.b).
- Also, the value of  $q_{c5} < q < q_{c6}$  and  $d_{56} < 0, p_{56} = 0$ , unstable saddle nodes are the slump point, see Figure (5.c).

Bifurcation schemes in the (y-q) level for different values of the phase differences of (ratios of amplitude, magnetic field and inclined angle) in Figure 5(ia, iib, iiic).

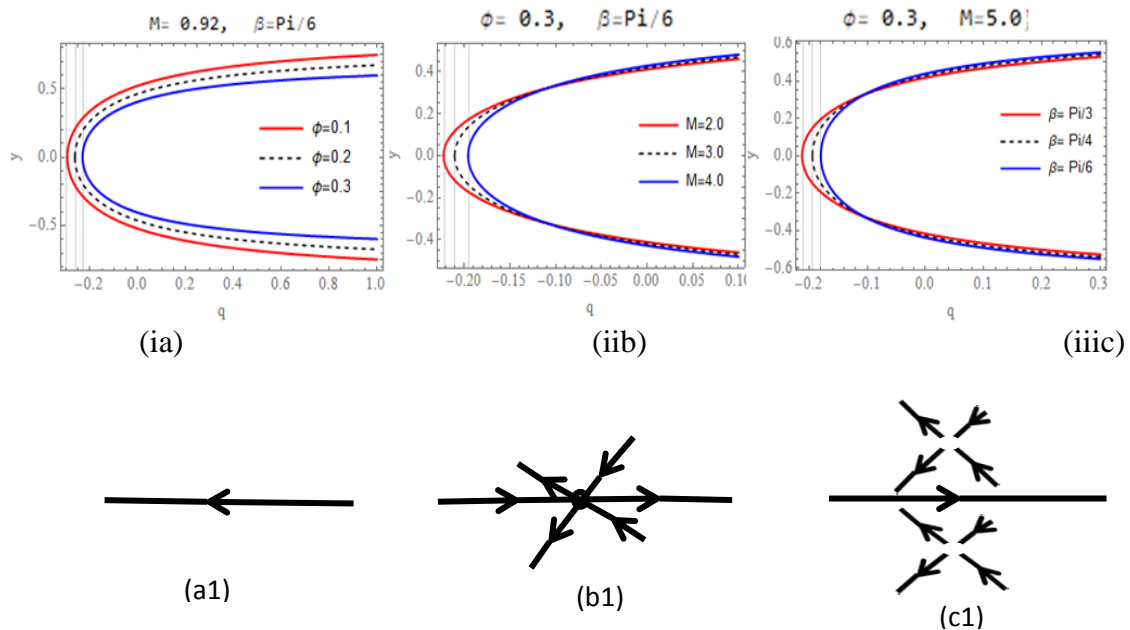


**Figure 5:** Diagrams of bifurcations (ia, iib, iiic) at  $x = x_{5,6}$  and topological variations (a1)  $q > q_{c5}$ , (b1)  $q = q_{c5} = q_{c6}$ , (c1)  $q_{c5} < q < q_{c6}$

**6. Stream styles and global bifurcation**

The vector field that is limited to this branch when  $y=0$  is  $\{\dot{x}, \dot{y}\} = \left\{ \frac{\sqrt{A}(-q-h+q\text{Cosh}[\sqrt{A}h])+\text{Sinh}[\sqrt{A}h]}{\sqrt{A}h\text{Cosh}[\sqrt{A}h]-\text{Sinh}[\sqrt{A}h]}, 0 \right\}$ , from which

$$\xi = \frac{\sqrt{A}(-q-h+q\text{Cosh}[\sqrt{A}h])+\text{Sinh}[\sqrt{A}h]}{\sqrt{A}h\text{Cosh}[\sqrt{A}h]-\text{Sinh}[\sqrt{A}h]}$$

develop. Since  $\xi = 0$  determines the global bifurcation curves, we obtain

$$\xi|_{(x=n\pi)} = \frac{\sqrt{A}(-1-F+F\text{Cosh}[\sqrt{A}])+\text{Sinh}[\sqrt{A}]}{\sqrt{A}\text{Cosh}[\sqrt{A}]-\text{Sinh}[\sqrt{A}]} = 0,$$

$$\xi|_{(x=\frac{(2n-1)\pi}{2})} = \frac{\sqrt{A}(-1-q+\phi+q\text{Cosh}[\sqrt{A}(1-\phi)])+\text{Sinh}[\sqrt{A}(1-\phi)]}{\sqrt{A}(1-\phi)\text{Cosh}[\sqrt{A}(1-\phi)]-\text{Sinh}[\sqrt{A}(1-\phi)]} = 0.$$

The parameters' global bifurcation diagram  $\phi - q$  comprises the following set curves with a variation of A:

$$M = \{(\phi, q) | 0 < \phi < 1, q = \frac{1 - \frac{\text{Sinh}[\sqrt{A}]}{\sqrt{A}}}{-1 + \text{Cosh}[\sqrt{A}]}\},$$

$$N = \{(\phi, q) | 0 < \phi < 1, q = -\frac{-1 + \phi + \frac{\text{Sinh}[\sqrt{A}(1-\phi)]}{\sqrt{A}}}{-1 + \text{Cosh}[\sqrt{A}(1-\phi)]}\}.$$

Along the bifurcation curve M, there exist isolated non-hyperbolic decadent points below the wave crests that are also non-simple. Whereas along bifurcation curve N, the related critical points connect in non-simple degenerate point connections underneath the wave troughs. Six heteroclinic pathways exist at critical locations that merge on a deteriorated saddle based on the N product. Curves that bifurcate are shown in Figure (6). These are the divisions of the peristaltic flow region:

Region I: backward flow, in which all of the flow is going the other way.

Region II: trapping occurs when two vortices with opposing rotations interact and the saddle are connected by heteroclinic connections.

Region III: Augment flow, in which some of the fluid is able to pass through the centreline in the flow direction and eddies below wave crests combine to establish heteroclinic linkages with their neighbours.

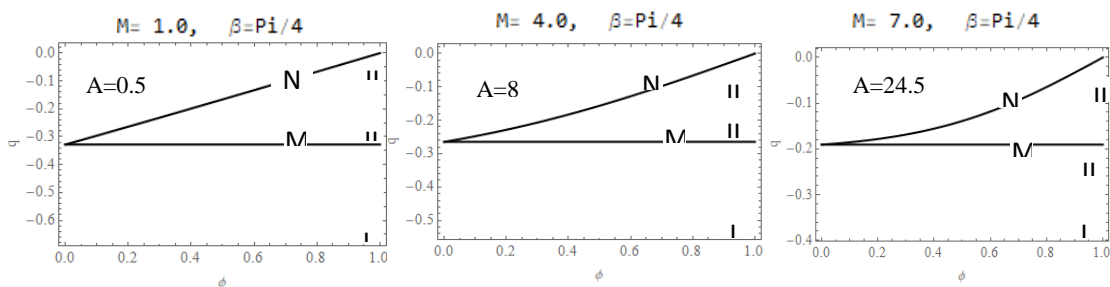


**Figure 6:** Global bifurcation for a planar change of A with distinct regions I for backward flow, II for trapping, and III for augmented flow.

**7. Discussion of the findings**

It is crucial to clarify the importance of the current work for practical applications. Peristalsis allows for the construction of pumps without any moving components, such as valves, plungers, or rotors, coming into contact with the fluid being transported. In Figure (2) we notes that the three move of the flow, when give different values of q (backward, trapping and augmented). The stability of the equilibrium points and streamline topologies of different flow scenarios, as well as their bifurcations, are investigated in Figures (3, 4, 5, 6). Notes that in Figure (3), we explore the first flow field bifurcation and demonstrates the stability case of stagnation sites which are located on a vertical line between the upper and lower walls of the

channel, expressing the kind and stability of equilibrium points as  $\{x_{1,2}, y_{1,2}\}$  are expressed, see Figures 3(a1,a2,a3). Once  $q$  crosses through the critical values with a transverse orientation, an unstable saddle on the centerline separates into two stable centers. By increasing the amplitude ratio, magnetic field, and inclination angle, the bifurcation point changes from positive to negative transverse flow directions by widening the phase differences, see Figure (3).

Figure (4) illustrates the characteristics and stability of the crucial points  $\{x_{3,4}, y_{3,4}\}$  and explains how the saddle splits into saddle nodes, which straighten the center in the longitudinal direction. It submits that by reducing the amplitude ratios and magnetic field. Both longitudinally and transversely, the eddying zone expands, while the opposite for inclined angles. It should be noticed that for high phase differences, the saddle nodes migrate swiftly in the direction of their nearby stagnation points. When  $q$  approaches the second critical value  $q_{c_2}$ , these saddle nodes merge between the wave trough of the upper and lower walls of the channel to produce non-simple decadent points on the centerline bind with six heteroclinic connections, see Figures (4a, 4b, 4c).

Figure (5) illustrates the bifurcation of decadent points into saddle nodes in an episodic direction is shown by the type and stability of equilibrium point  $\{x_{5,6}, y_{5,6}\}$ . Figure (5) illustrates how this bifurcation manifests at low flow rate for big ratios of amplitude. The vertical direction of the distance between saddle nodes shows an increase by a reduction in amplitude ratios, inclined angle and magnetic field, see Figure 5(a, b, c).

In Figure (6), we display diagrams of global bifurcation for various values of  $A$ , it is observed that as the value of  $A$  rises, so it does the range of  $q$  where trapping occurs. We also see that trapping and argument enhance the curvature of the curve as the value of  $A$  rises, and they start to stay together before separating.

## 8. Conclusion

In this research, we investigated at how magnetic field and inclined angle affected streamline styles and their bifurcations in two-dimensional, symmetric canal Newtonian fluid flow hence the most likely equilibrium points are in the saddle or in the middle. By looking at the eigenvalues of the Jacobian matrix, the critical locations were identified. This approach was used until it was determined for several flow conditions the local bifurcation of the obverse equilibrium points took place. There are three different flow instances that can express themselves: (backward, trapping, and augmented flow). Key conclusions from the research include the following:

- A- The manifestation of the following three flow cases, namely the Augmented, backward, and trapping flows have all been identified.
- B- The backward region retracts when the  $q$  is raised to its highest value, and the opposite behaviour is observed.
- C- A higher amplitude value suggests that there are more blouses, less trapping, additionally, that they are nearer the centerline.
- D- The arrival amplitude ratio's mention of the best value suggests that there are more blouses along the channel walls.
- E- Saddle, Saddle or center nodes are positioned on the center line, below the wave peaks, and through the channel walls.

## References

- [1] Shapiro AH, Jaffrin MY, Weinberg SL, (1969), "Peristaltic pumping with long wavelengths at low Reynolds number", *J Fluid Mech* 37:799–825.

- [2] Hatem Nahi Mohaisen, Ahmed M.Abedulhadi (2022) , “Influence of the Induced Magnetic and Rotation on Mixed Convection Heat Transfer for the Peristaltic Transport of Bingham plastic Fluid in an Asymmetric Channel”, *Iraqi Journal of Science*, Vol. 63, No. 4, PP: 1770-1785, DOI: 10.24996/ij.s.2022.63.4.35.
- [3] S. Nadeem, Safia Akram , (2010), “Influence of inclined magnetic field on peristaltic flow of a Williamson fluid model in an inclined symmetric and asymmetric channel”, *Mathematical and Computer Modelling*, 52, PP: 107-119.
- [4] Farah Alaa Adnan, Ahmad M. Abdul Hadi, (2019), “Effect of an inclined magnetic field on peristaltic flow of Bingham plastic fluid in an inclined symmetric channel with slip conditions”, *Iraqi Journal of Science*, Vol. 60, No.7, PP: 1551-1574 DOI: 10.24996/ij.s.2019.60.7.16.
- [5] Kaleem Ullah, Nasir Ali, Muhammad Sajid, (2019), “Bifurcation and stability analysis of critical/stagnation points for peristaltic transport of a power-law fluid in a tube”, *Journal of the Brazilian Society of Mechanical Sciences and Engineering* 41:420 <https://doi.org/10.1007/s40430-019-1910-9>.
- [6] F. G URCAN, A. D E L ICEO GLU AND P. G. B A K K E R, (2005), “Streamline topologies near a non-simple degenerate critical point close to a stationary wall using normal forms”, *J. Fluid Mech*, vol. 539, pp. 299–311, doi:10.1017/S0022112005005689.
- [7] F. Gürcan and A. Deliceoğlu, (2005), “Streamline topologies near nonsimple degenerate points in two-dimensional flows with double symmetry away from boundaries and an application ”, *Physics of Fluids*, Volume 17, Issue 9, <https://doi.org/10.1063/1.2055527>.
- [8] MORTEN BRØNS, (2007), “Streamline Topology: Patterns in Fluid Flows and their Bifurcations”, *Advances in Applied Mechanics*, Volume 41, PP: 1-42.
- [9] A. D E L ICEO GLU AND F. G URCAN, (2008), “Streamline topology near non-simple degenerate critical points in two-dimensional flow with symmetry about an axis ”, *J. Fluid Mech.* (2008), vol. 606, pp. 417–432, doi:10.1017/S0022112008001997.
- [10] Joel Jiménez-Lozano, Mihir Sen, (2010), “Streamline topologies of two-dimensional peristaltic flow and their bifurcations”, *Chemical Engineering and Processing vol.49*, doi:10.1016/j.cep.2009.10.005.
- [11] Z. Asghar and N. Ali, (2015), “Streamline topologies and their bifurcations for mixed convective peristaltic flow “, *AIP Advances* , Vol. 5, Issue 9, <http://dx.doi.org/10.1063/1.4931088>.
- [12] Ullah, Kaleem; Ali, Nasir (2019), “ Stability and bifurcation analysis of stagnation/equilibrium points for peristaltic transport in a curved channel”, *Physics of Fluids*, Vol. 31 Issue 7, doi:10.1063/1.5097555
- [13] Sadia Waheed, Anber Saleem, S. Nadeem (2019), “Physiological analysis of streamline topologies and their bifurcations for a peristaltic flow of nano fluid”, *Microsystem Technologies*, Vol. 25, No. 4, pp: 1267–1296, <https://doi.org/10.1007/s00542-018-4154-1>.
- [14] Nasir Ali, Kaleem Ullah and Husnain Rasool (2020), “Bifurcation analysis for a two-dimensional peristaltic driven flow of power-law fluid in asymmetric channel”, *Phys. Fluids* 32, 073104, <https://doi.org/10.1063/5.0011465>.
- [15] T. Ehsan, S. Asghar, and H. J. Anjum, (2020), “Identification of trapping in a peristaltic flow: A new approach using dynamical system theory”, *Phys. Fluids* 32, 011901; doi: 10.1063/1.5128417.
- [16] V. Jagdeesh, S.Sreenadh, P. Lakshminarayana, (2018), “Influence of Inclined Magnetic Field on the Peristaltic Flow of a Jeffrey Fluid in an Inclined Porous Channel”, *International journal of Engineering & Technology* 7(4.10) pp:319-322, [www.sciencepubaco.com/Lindex.php/LIJET](http://www.sciencepubaco.com/Lindex.php/LIJET).
- [17] Kaleem Ullah, Nasir Ali, and Sadaqut Hussain, (2021),” Bifurcation analysis for a flow of viscoelastic fluid due to peristaltic activity”, *Phys. Fluids* 33, 053101, <https://doi.org/10.1063/5.0049251>.
- [18] A.M. Siddiqui, W.H. Schwarz,(1994), “Peristaltic flow of a second-order fluid in tubes ”, *Journal of Non-Newtonian Fluid Mechanics*,53, PP:257-284.
- [19] Bakker P.G. (1991), “Bifurcation in Flow Patterns”, Dordrech: Kluwer Academic Publishers.
- [20] Seydel R., (1988), “From Equilibrium to Chaos: Practical Bifurcation and Stability Analysis”, New York: Elsevier.